Phase diagrams and physical properties of binary ferroelectric mixtures based on a series of chiral α-cyanocinnamate derivatives

A. Vajda, M. Kaspar, V. Hamplova, A. Bubnov, K. Fodor-Csorba & N. E ber

PLEASE SCROLL DOWN FOR ARTICLE

Phase diagrams and physical properties of binary ferroelectric mixtures based on a series of chiral α-cyanocinnamate derivatives

A. VAJDA*, M. KASPAR†, V. HAMPLOVA†, A. BUBNOV†,
K. FODOR-CSORBA and N. ÉBER

Research Institute for Solid State Physics and Optics of the Hungarian Academy
of Sciences, H-1525 Budapest, P.O.B. 49, Hungary
†Institute of Physics, Academy of Sciences of the Czech Republic, Na Slovance 2,
18221 Prague 8, Czech Republic

We report a detailed investigation of binary mixtures composed of members of the homologous series of (*S*)-4′-(2-*n*-alkoxypropanoyloxy)biphenyl-4-yl 4-*n*-alkoxy-α-cyanocinnamates. The phase transition curves for these mixtures have no minima. On the contrary, eutectic behaviour was obtained if the members of this homologous series were mixed with structurally different chiral cinnamic acid derivatives and other ferroelectric liquid crystal materials. Spontaneous polarization, tilt angle and dielectric constant results were obtained for three of the single compounds and nine ferroelectric mixtures.

1. Introduction

Ferroelectric liquid crystals have attracted great attention in recent decades due to their ability to give fast electro-optical switching [1, 2]. Numerous compounds have been synthesized in order to obtain a well defined set of physical and physico-chemical properties such as high chemical stability, wide temperature range of the chiral smectic C (SmC*) phase, appropriate values of the spontaneous polarization and tilt angle, and a low viscosity. The properties can be further modified by preparation of mixtures [3]. Usually, these new properties cannot be predicted precisely on the basis of the liquid crystalline properties of the individual compounds. To our best knowledge, no results have been published on the mixtures formed from α-cyanocinnamate derivatives. In the following investigations we have pointed out the importance of variation of the electronic structure of the chiral compounds and its influence on the mesomorphic behaviour as indicated in [4].

(*R*)- or (*S*)-*O*-alkyl lactates are convenient starting materials for the synthesis of chiral liquid crystals. Many of their derivatives possessing different core systems have already been prepared and shown to exhibit ferroelectric switching and a high spontaneous polarization [5–7]. Recently the homologous series of (*S*)-4′-(2-*n*-alkoxypropanoyloxy)biphenyl-4-yl 4-*n*-alkoxy-α-cyanocinnamates was synthesized and characterised [8]. All these compounds showed the SmC* phase at high temperatures

and possessed large tilt angles of about 44 degrees. In our experiments the properties of these individual compounds were investigated and changed either by mixing them with other homologues or with cinnamate esters having the (*S*)-2-methylbutyl group as the chiral part. In order to investigate the space filling, some of these compounds were chosen to have an α-cyano group in their core system.

2. Experimental

The chemical purity of the individual compounds was determined by high performance liquid chromatography using an Ecom HPLC chromatograph and a silica gel column (Separon 7 μm, 3 × 350, Tessek) eluted with a mixture of 99.9% toluene and 0.1% methanol. The elution profile was checked by a UV-VIS detector working at $\lambda = 290$ nm. The chemical purity was in the range 99.1–99.8%.

The sequence of mesophases and the phase transition temperatures were determined by observing their characteristic textures in unoriented sandwich cells on heating and cooling cycles using an Amplival PolU polarizing microscope equipped with a Boetius hot-stage. The heating rate was $4°C\,min^{-1}$; the cooling rate was uncontrolled. The phase diagrams were determined by optical microscopy using first the contact method [9] and finally by the determination of the transition temperatures of selected mixtures of known concentration [10].

The physical measurements were performed on 25 μm thick planar samples in the bookshelf geometry.

*Author for correspondence; e-mail: vajda@szfki.hu

The spontaneous polarisation (P_s) of the substances was evaluated from the $P(E)$ hysteresis loop detected during switching in an a.c. electric field (E) at a frequency of 60 Hz. The tilt angle (θ_s) was determined optically from the difference between the extinction positions with crossed polarizers under application of opposite d.c. electric fields of $\pm$ 40 kV cm^{-1}. The real part of the dielectric permittivity (ε') was measured on cooling from the isotropic (I) phase at a frequency of 30 Hz using a Schlumberger 1260 impedance analyser.

The molecular geometries were optimized in the all-*trans*-conformation by the PM3 semiempirical quantum chemical method giving the molecular length (l) of the compounds investigated.

3. Results and discussion

3.1. *Binary mixtures, phase diagrams and miscibility studies*

The chemical structures and phase sequences of the individual compounds investigated in this work are summarized in the scheme. Binary mixtures composed of members of the homologous series of (S)-4'-(2-*n*-alkoxy-propanoyloxybiphenyl-4-yl 4-*n*-alkoxy-α-cyanocinnamates [n/m], e.g. 1 ($n/m = 12/10$), 2 ($n/m = 12/5$) and 3 ($n/m = 7/7$), in any combination possessed a ferroelectric SmC* phase. Figure 1 depicts the phase diagram for mixtures of 1 and 3. Those mixtures containing 3 in high concentration formed first a blue phase (BP), then a chiral nematic (N*) phase when cooling the isotropic (I) liquid. The mixtures of these individual homologues showed no tendency to form a minimum in their melting curve whether or not the chain length of the chiral or of the achiral parts of the molecule was varied.

The influence of additives with slightly or quite different chemical constitutions was investigated, keeping one representative of the above homologous series as a basic component of all binary mixtures. Having the lowest melting point and the widest range N* phase among these compounds, 3 was chosen as this representative.

The influence of three additives with the same chiral part, (S)-2-methylbutyl esters with slightly varied core systems, was tested first. Two of them were cinnamate

1 n = 12, m = 10   Cr 92 SmC* 141 I   [8]

2 n = 12, m = 5   Cr 93 SmC* 140 N* 144 I   [8]

3 n = 7, m = 7   Cr 89 SmC* 124 N* 138 BP 143 I   [8]

4   [11]

Cr 81 (SmC*76) SmA* 89 I

5   [12]

Cr 61 SmC* 70 SmA* 95 I

6   [13]

Cr 76 (SmF*60) SmC* 106 SmA* 153 I

7

Cr 95 (SmC*44) SmA* 142 N* 148 I
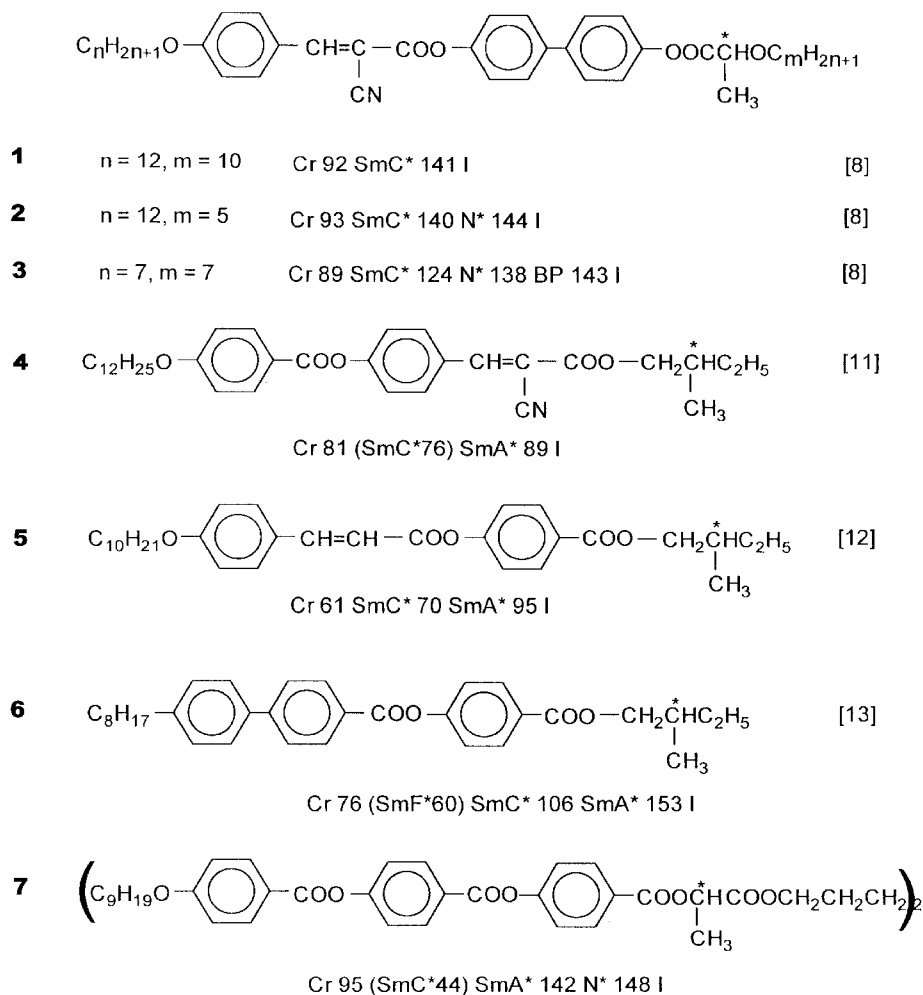
Scheme. Chemical structures and phase transitions of the liquid crystal materials used in the mixtures.
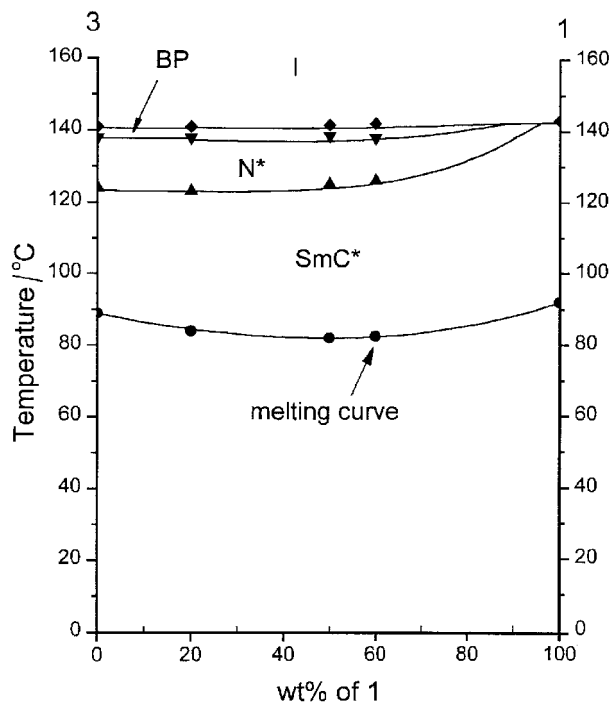
Figure 1. Phase diagram of binary systems composed of **1** and **3**.
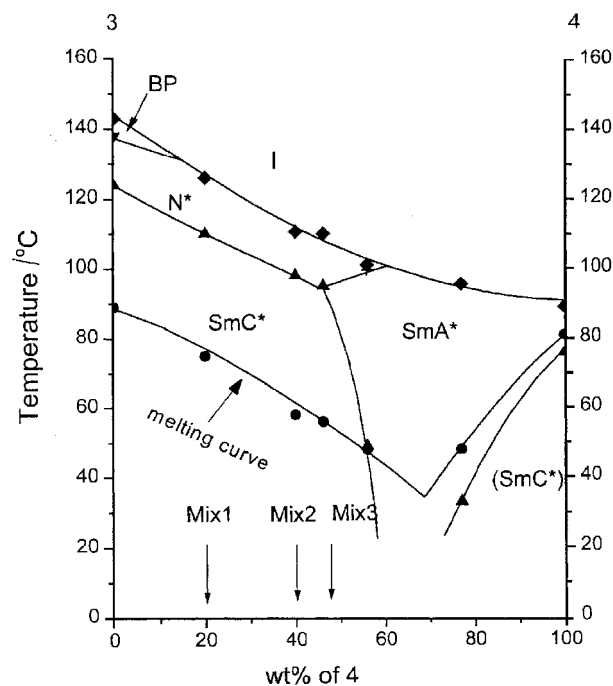
Figure 2. Phase diagram of binary systems composed of **3** and **4**.

derivatives, (*S*)-2-methylbutyl 4-(4-dodecyloxybenzoyl-oxy)-α-cyanocinnamate (**4**) [11] and (*S*)-2-methylbutyl 4-(4-decyloxycinnamoyloxy)benzoate (**5**) [12]. The third additive was a benzoate ester, namely (*S*)-2-methylbutyl 4-(4′-octylbiphenyl-4-carbonyloxy) benzoate (**6**) [13].

Figure 2 represents the phase diagram of the binary mixtures composed of **3** and **4**. The large perpendicular dipole moment of the cyano group in **4** is closer to the chiral centre than in **3**, though it still belongs to the core system owing to the extended delocalization of π-electrons. The cores of **3** and **4** are quite different sterically, and their miscibility was limited; in all mixtures, phase coexistence regions of several degrees were observed. The phase diagram showed eutectic behaviour. The composition at about a 1:1 ratio of the ingredients (Mix3) resulted in a readily supercooled SmC* phase. In the mixtures containing **3** in 80 wt % (Mix1) and 60 wt % (Mix2), the ranges of both the N* and SmC* phases were broadened slightly compared with those for the individual material **3**.

The additive **5** is also a cinnamic acid derivative, but in contrast to **4** it does not contain the large perpendicular dipole of the cyano group in its core system. Compounds **3** and **5** provided a similar phase diagram to that in figure 2, though phase coexistence regions were not detected. These compositions also gave a eutectic behaviour around the 1:1 ratio, but the SmC* phase became monotropic at this concentration. The

mixtures containing **5** in 60–70 wt % (figure 3) melted at considerably lower temperatures compared with those of the individual components and the SmC* phase could
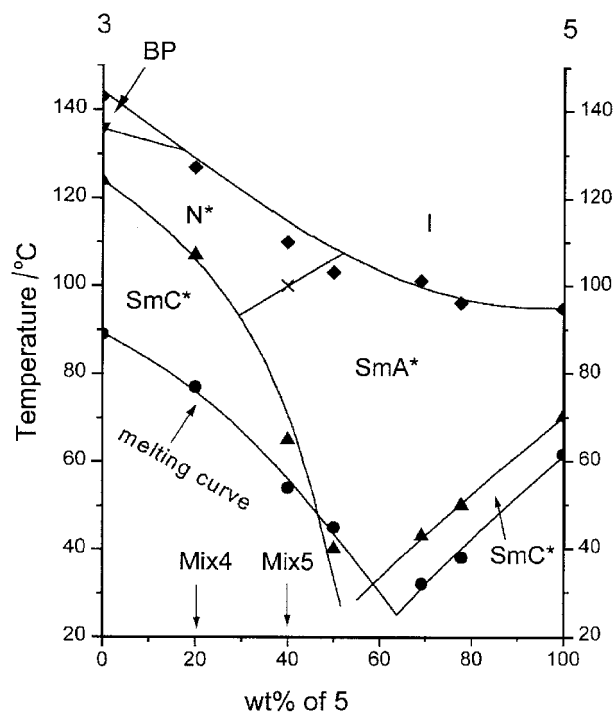
Figure 3. Phase diagram of binary systems composed of **3** and **5**.

be supercooled far below room temperature. Blue phase formation was not observed in any mixture.

The core geometry of the additive **6** differs significantly from that of the basic component **3**, as it lacks the α-cyanocinnamate bridging group. Moreover, the biphenyl group is connected to the achiral chain instead of the chiral chain. The mixtures of **3** and **6** exhibited quite different phase sequences compared with that of the individual compounds, as shown in figure 4. The blue and SmF* phases of the individual compounds were completely eliminated in all the mixtures investigated (figure 4). An increasing concentration of **6** first resulted in the shift of the SmC* temperature range to lower temperatures while the initial broadening of the N* range (Mix6) became a narrowing after the appearance of the SmA* phase (Mix7). The melting curve showed eutectic behaviour. In the mixtures where **6** is present in 60–80 wt %, in the neighbourhood of the eutectic concentration, the SmA* phase of both compounds was strongly broadened. The SmA*–SmC* transition was shifted far below the melting temperature. These compositions were frozen out from the SmC* phase at about -30°C.

A new series of bimesogenic compounds has been prepared in our laboratories. One representative of this series bis-1,6-[(*S*)-2-{4-[4-(4-nonyloxyphenylcarbonyloxy)-phenylcarbonyloxy] phenylcarbonyloxy}propanoyloxy]-hexane (**7**) was added to **3**. Both compounds have the

same chiral centre. In the bimesogen the chiral parts are connected by the spacer so they are situated inside the molecule, while in **3** the chiral part is a terminal group. The melting of these mixtures showed eutectic behaviour. In all the mixtures investigated, enantiotropic BP and N* phases were observed. The same holds for the SmC* phase except for the highest concentrations of **7**. A minimum point in the N* phase appeared at about a 25 wt % concentration of **7**. With an increasing amount of **7**, the SmA* phase became dominant (figure 5). The SmA*–SmC* phase transition temperature showed a slight monotonic decrease with increasing concentration of **7** and all mixtures were readily supercooled below 0°C.

The calculated molecular geometries and the resulting molecular lengths for compounds **1**–**7** in their all-*trans* conformations are summarized in figure 6. In the phase diagrams shown in figures 2–4 a strong tendency can be seen to form minima in the melting curves and the transition curves between different mesophases. Though the molecular lengths of compounds **3**–**6** are roughly similar, their different core systems do not allow very close stacking, which might be the reason for the limited miscibility. In a narrow concentration range, however, the SmC* phase could be shifted far below the melting points of the individual compounds. No minima were obtained when members of the same homologous series were mixed (figure 1) as the identical core systems do not hinder the close packing of the molecules. The
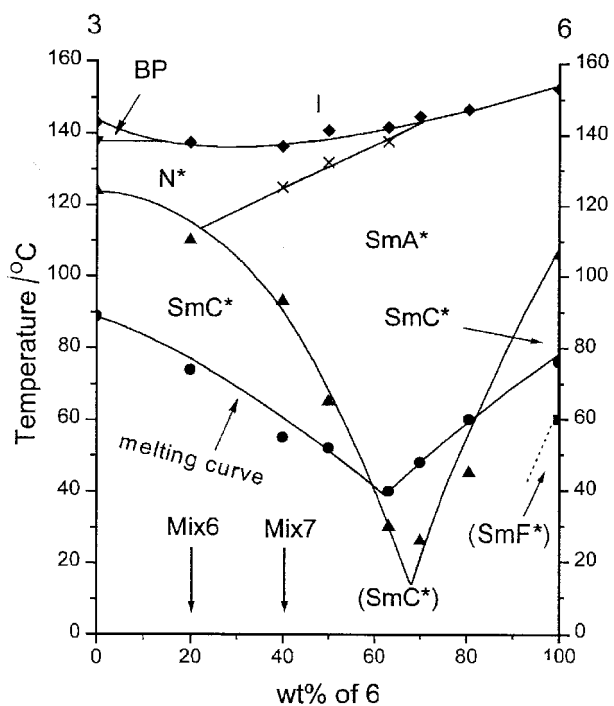
Figure 4.   Phase diagram of binary systems composed of **3** and **6**.
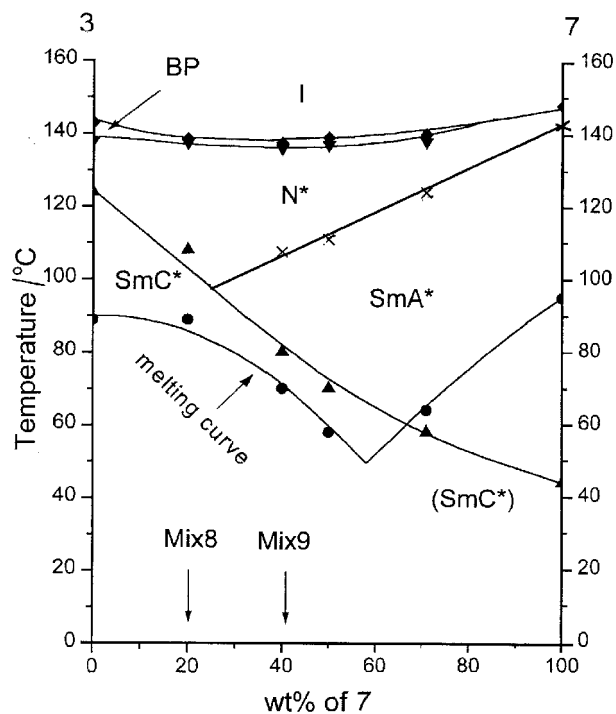
Figure 5.   Phase diagram of binary systems composed of **3** and **7**.

compound	conformer	length (Å)
1		49.60
2		43.54
3		40.09
4		36.16
5		33.61
6		31.63
7		75.57
3+7		40.09
		75.57
		40.09
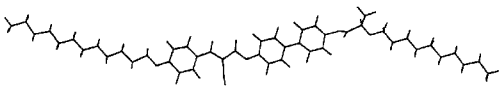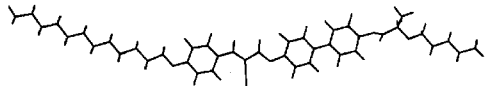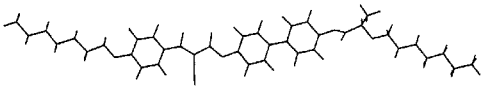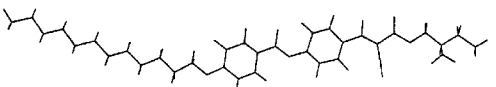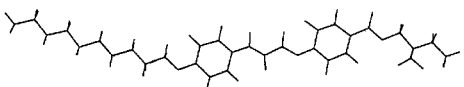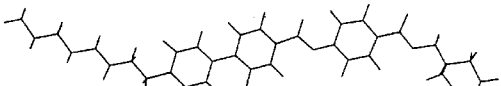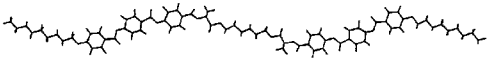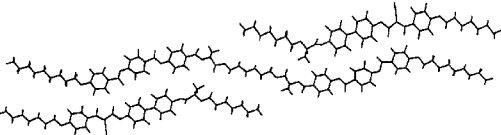
Figure 6. The all-*trans*-conformers of the liquid crystal materials calculated by the PM3 method.

phase diagram depicted in figure 5 represents a situation between these two kinds of behaviour, where the melting curve and the N* phase have minimum points, but the SmA*–SmC* phase transition temperature decreases almost linearly. The large difference in the molecular lengths (75.57 Å of **7** in contrast to 40.09 Å of **3**) allows a possible close stacking of these two compounds, where two of the relatively 'short' molecules of **3** can be oriented along the length of the bimesogen as shown in figure 6. X-ray investigations are in progress.

Table 1.   Phase sequences for the binary ferroelectric mixtures.

Mixtures	Composition/wt %					Phase sequence/°C
	3	4	5	6	7	
Mix1	80	20	—	—	—	Cr ~76 SmC* 111 N* 128 I
Mix2	60	40	—	—	—	Cr ~60 SmC* 99 N* 110.5 I
Mix3	53.8	46.2	—	—	—	Cr ~56 SmC* 97 N* 110 I
Mix4	80	—	20	—	—	Cr ~77 SmC* 107 N* 127 I
Mix5	60	—	40	—	—	Cr ~55 SmC* 66 SmA* 100 N* 111 I
Mix6	80	—	—	20	—	Cr ~74 SmC* 110 N* 138 I
Mix7	60	—	—	40	—	Cr ~55 SmC* 93 SmA* 125 N* 136.5 I
Mix8	80	—	—	—	20	Cr ~89 SmC* 108 N* 138 BP 139.5 I
Mix9	60	—	—	—	40	Cr ~70 SmC* 80 SmA* 108 N* 137 BP 138 I

3.2. *Spontaneous polarization, tilt angle, and dielectric permittivity*

For further characterization of their ferroelectric properties, at least two mixtures have been selected from each of the phase diagrams (those with 80 and 60 wt % of **3**). The composition and the phase sequences of these mixtures are summarized in table 1.

The spontaneous polarization, tilt angle and dielectric permittivity of each of these mixtures and of some individual compounds were measured over the full temperature range of the SmC* phase. The P_s and θ_s values measured 10 and 20°C below the paraelectric–ferroelectric phase transition temperature (T_c) are tabulated in table 2, while figures 7(*a*) and 8(*a*) show some examples of the whole temperature dependence for the mixtures indicated. The curves indicate two clearly distinguishable behaviours which correlate well with the nature of the paraelectric–ferroelectric transition.

The individual lactates (e.g. **3**) have a nearly temperature-independent tilt angle of about $\theta_s \approx 43.0$–$44.7°$,

Table 2.   Spontaneous polarisation P_s (nC cm^{-2}) and tilt angle θ_s (°) measured at 10°C and 20°C below the temperature (T_c) of the phase transition to the SmC* phase on cooling.

Sample	P_s ($T_c - 10°C$)	P_s ($T_c - 20°C$)	θ_s ($T_c - 10°C$)	θ_s ($T_c - 20°C$)
Mix1	65	73	35	36
Mix2	46	55	31	33
3	34	42	29	31
3	78	83	41	43
Mix4	44	61	33	35
Mix5	26	36	18	23
5	12	14	21	24
Mix6	47	91	34	36
Mix7	48	54	17	19
6	5	6	14	19
Mix8	66	81	32	36
Mix9	23	33	20	23
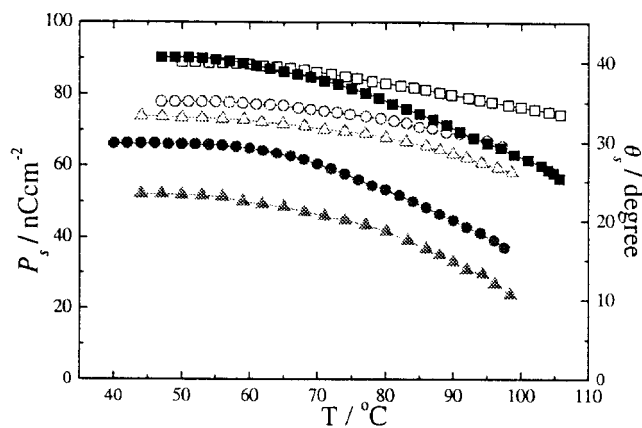
(*a*)
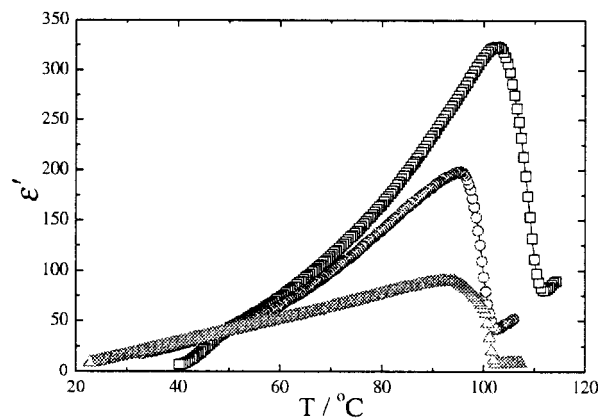
(*b*)

Figure 7.   (*a*) Temperature dependence of the spontaneous polarization (solid symbols) and tilt angle (open symbols) for Mix1 (squares), Mix2 (circles) and Mix3 (triangles). (*b*) Temperature dependence of the real part of complex permittivity at 30 Hz for Mix1 (squares), Mix2 (circles) and Mix3 (triangles).

(a)

(b)
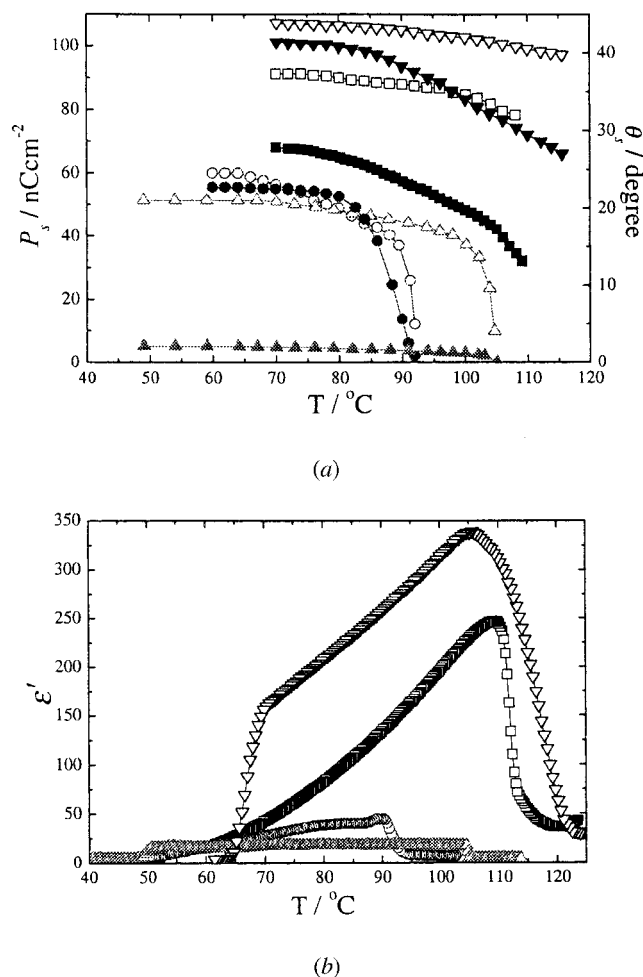
Figure 8. (a) Temperature dependence of the spontaneous polarization (solid symbols) and tilt angle (open symbols) for Mix6 (squares), Mix7 (circles), **3** (inverted triangles) and **6** (triangles). (b) Temperature dependence of the real part of the complex permittivity at 30 Hz for Mix6 (squares), Mix7 (circles), **3** (inverted triangles) and **6** (triangles).

which together with their P_s drops to zero at T_c. Such a behaviour is quite typical for substances possessing a strongly first order SmC*↔N* phase transition. Similar behaviour holds for mixtures with the same phase sequence (Mix1, Mix2, Mix3, Mix4, Mix6, Mix8), though the temperature dependence of the tilt and polarization becomes there slightly more pronounced.

Two additives (**5** and **6**) with a second order SmC*↔ SmA* phase transition behaved regularly with a continuously falling P_s and θ_s when approaching T_c. The same applied for the mixtures Mix5, Mix7 and Mix9 where the high additive contents led to the appearance of the SmA* phase. The two other additives, **4** and **7** are also expected to behave similarly, but their polarization and tilt could not be measured due to their short range monotropic SmC* phase.

The spontaneous polarization, as well as the tilt angle, varied monotonically with concentration of the additives in all mixtures studied. Therefore, mixing could provide an effective tool for reducing the unwanted high tilt of **3** to $\theta_s \approx 19°$ for Mix7 and $\theta_s \approx 23°$ for Mix9.

Figures 7(b) and 8(b) present some examples of the temperature dependence of the real part ε' of the complex permittivity. Measured in the bookshelf geometry, the large ε' values in the SmC* phase represent the contribution of the Goldstone mode indicating the presence of a helical structure. Within all series of mixtures the dielectric constant decreases with decreasing amount of **3**. The soft mode contributions which are expected to appear in the form of small peaks near the SmC*–N* (or SmC*–SmA*) phase transitions could not be detected.

In the SmA*, N* and I phases the permittivity should drop to low values due to the lack of ferroelectric contributions. The still unusually large ε' values measured at high temperatures might be due to the relatively high conductivity of the substances originating from **3** or to other parasitic effects connected with the capacitance and the resistance of the surface (e.g. the polyimide) layers which are expected to diminish at higher frequencies ($\sim 1\,\text{kHz}$) only.

4. Conclusions

The α-cyanocinnamates gave no minima in their phase transition curves when mixtures were composed of other members of the homologous series independently of whether the alkyl chain length was even or odd numbered. The very long bimesogen **7** can host the short molecule of **3** and the cores can align almost parallel according to the calculations. The thermodynamically stable orthogonal phases became dominant probably due to this orientation. Numerous mixtures were found for combinations of **3** with **4**, **5**, **6** and **7** where the temperature range of the tilted SmC* phase was observed far below the melting curve. The mixtures investigated here exhibited a rather broad temperature interval of the ferroelectric phase. The P_s in the SmC* phase was relatively high and reached values up to $90\,\text{nC cm}^{-2}$ for some of the mixtures.

References

[1] LAGERWALL, S. T., 1999, *Ferroelectric and Antiferroelectric Liquid Crystals* (New York: Wiley-VHC, Weinheim) and references therein.

[2] BAHADUR, B., 1990, *Liquid Crystals: Applications and Uses*, Vol. 1 (Singapore: World Scientific) and references therein.

[3] DABROWSKI, R. S., SZULC, J., and SOSNOWSKA, B., 1992, *Mol. Cryst. liq. Cryst.*, **215,** 13.

[4] GOODBY, J. W., BLINC, R., CLARK, N. A., LAGERWALL, S. T., OSIPOV, M. A., PIKIN, S. A., SAKURAI, T., YOSHINO, K., and ZEKS, B., 1991, *Ferroelectric Liquid Crystals: Principles, Properties and Applications* (Philadelphia: Gordon and Breach).

[5] KASPAR, M., GLOGAROVA, M., HAMPLOVA, V., SVERENYAK, H., and PAKHOMOV, S. A., 1993, *Ferroelectrics*, **148,** 103.

[6] TSAI, W. L., and KUO, H. L., 1993, *Liq. Cryst.*, **13,** 765.

[7] KASPAR, M., GORECKA, E., SVERENYAK, H., HAMPLOVA, V., GLOGAROVA, M., and PAKHOMOV, S. A., 1995, *Liq. Cryst.*, **19,** 589.

[8] KASPAR, M., SVERENYAK, H., HAMPLOVA, V., PAKHOMOV, S. A., and GLOGAROVA, M., 1995, *Mol. Cryst. liq. Cryst.*, **260,** 241.

[9] SACKMANN, H., and DEMUS, D., 1973, *Mol. Cryst. liq. Cryst.*, **21,** 239.

[10] DEMUS, D., 1976, *Non-emissive Electrooptic Displays*, edited by A. R. Kmetz and F. K. von Willisen (New York: Plenum Press), pp. 92–98.

[11] LESLIE, T. M., 1984, *Ferroelectrics*, **58,** 9.

[12] GOODBY, J. W., and LESLIE, T. M., 1984, *Mol. Cryst. liq. Cryst.*, **110,** 175.

[13] COATES, D., 1987, *Liq. Cryst.*, **2,** 63.